RESEARCH PAPER

Nanomedicines of Hedgehog Inhibitor and PPAR-γ Agonist for Treating Liver Fibrosis

Virender Kumar • Vaibhav Mundra • Ram I. Mahato

ABSTRACT

Purpose Hedgehog (Hh) and peroxisome proliferator-activated receptor gamma (PPAR-γ) are major signaling pathways involved in the pathogenesis of liver fibrosis. Since Hh inhibitor, vismodegib (GDC) and PPAR-γ agonist, rosiglitazone (RSG) have poor water solubility, our objective was to formulate biodegradable polymeric nanoparticles encapsulating GDC and RSG for treating liver fibrosis.
Methods Methoxy-polyethylene-glycol-b-poly(carbonate-co-lactide) [mPEG-b-p(CB-co-LA)] was synthesized and characterized using ^{1}H NMR. Nanoparticles were prepared using this polymer by emulsification/solvent evaporation method to encapsulate GDC and RSG either alone or in combination. Nanoparticles were characterized for particle size, drug loading, drug release, and anti-fibrotic efficacy after tail vein injection into common bile duct ligated (CBDL) fibrotic rats.
Results mPEG-b-p(CB-co-LA) copolymer has molecular weight of 30,000 Da as determined by ^{1}H NMR. Nanoparticles were monodisperse with a mean particle size of 120–130 nm. Drug loading was 5% and 2% w/w for GDC and RSG, respectively. Nanoparticles carrying both GDC and RSG were formulated at half of their individual drug loading. Systemic administration of drug loaded nanoparticles protected liver injury in CBDL rats by suppressing the activation of hepatic stellate cells, and decreasing inflammatory cytokines.
Conclusion Polymeric nanoparticles for co-delivery of Hh inhibitor and PPAR-γ agonist have the potential to treat liver fibrosis by intervening complex fibrotic cascade.

V. Kumar • V. Mundra • R. I. Mahato
Department of Pharmaceutical Sciences
University of Tennessee Health Science Center
Memphis, Tennessee 38163, USA

R. I. Mahato (✉)
Department of Pharmaceutical Sciences
University of Nebraska Medical Center (UNMC)
986025 Nebraska Medical Center
Omaha, Nebraska 68198-6025, USA
e-mail: ram.mahato@unmc.edu

ABBREVIATIONS

ALT	serum alanine transaminase
AST	serum aspartate transaminase
CBDL	common bile duct ligation
EMT	epithelial to mesenchymal transition
GDC	vismodegib
Hh	Hedgehog
HSCs	hepatic stellate cells
IL-6	interleukin-6
mPEG-b-p(CB-co-LA)	Methoxy-polyethylene-glycol-b-poly (carbonate-co-lactide)
NFκB	nuclear factor κB
PPAR-γ	peroxisome proliferator-activated receptor gamma
Ptch-1	Patched-1
ROS	reactive oxygen species
RSG	rosiglitazone
Shh	Sonic hedgehog
TGF-β1	transforming growth factor beta 1
TNF-α	tumor necrosis factor α

INTRODUCTION

Liver fibrosis is a pathological condition characterized by liver inflammation, which activate hepatic stellate cells (HSCs) and overproduce extra cellular matrix (ECM). Progression of liver fibrosis may results in cirrhosis which is associated with significant morbidity and mortality worldwide. Upon liver injury, damaged hepatocytes and other surrounding cells in the liver secrete multiple signaling molecules and inflammatory cytokines including hedgehog (Hh) ligand, transforming growth factor beta 1 (TGF-β1), platelet derived growth factor beta

(PDGF-β), interleukin 6 (IL-6) and tumor necrosis factor alpha (TNF-α) (1). Hh pathway plays an important role in the construction and remodeling of injured tissues (2). Hh ligand initiates smoothened (SMO) mediated signaling to activate Gli family transcription factors. Activation of Gli results in induction of epithelial to mesenchymal transition (EMT) which is a key event in the initiation and progression of fibrosis (3). Upon activation, HSCs lose PPAR-γ, a nuclear family receptors, which maintain the quiescent state of HSCs through dimerization with liver X receptor-α and alters the transcription of numerous genes including PDGF-β, TNF-α and TGF-β1 (4,5).

Although much is known about the molecular basis and pathophysiology of liver fibrosis, successful application of new therapeutic approaches is limited. Thus, there is an urgent need to develop alternative and effective treatment for liver fibrosis. Common bile duct ligation (CBDL) activates HSCs and increases the expression of patched homologue 1 (Ptch-1), sonic hedgehog (Shh) and Gli-1, but down regulates PPAR-γ expression (6,7). We have recently shown that Hh inhibitors such as cyclopamine and vismodegib (GDC) can significantly reduce the progression of liver fibrosis induced by CBDL in rats (8,9). Treatment with PPAR-γ agonist rosiglitazone (RSG) inhibits HSC activation and inflammatory pathways such as nuclear factor κB (NFκB), IL-6, and TNF-α (10).

Since GDC has anticancer activity and RSG causes cardiac complications, the purpose of this study was to determine whether we can treat liver fibrosis by co-delivery of these two drugs at the half of their individual doses (11,12). Since these two drugs are poorly soluble in water and RSG has short half-life, we decided to encapsulate them into biodegradable nanoparticles. Since nanoparticles can improve their pharmacokinetic profiles and reduce their side effects, we first synthesized methoxy-polyethylene-glycol-b-poly(carbonate-co-lactide)[mPEG-b-P(CB-co-LA)] copolymer and characterized it by ^{1}H NMR. Nanoparticles were characterized for particle size distribution, drug loading, and drug release. Anti-fibrotic properties of the formulations were determined by measuring the levels of Hh ligands, PPAR-γ and other fibrosis related markers in normal and CBDL rats after systemic administration of nanoparticles loaded with GDC and RSG as a single drug or both at half of their individual doses. Our main objective was to determine whether the combination treatment even at half dose can provide hepatoprotection and treat liver fibrosis.

MATERIALS AND METHODS

Materials

2, 2-Bis (hydroxymethyl) propionic acid, methoxy poly (ethylene glycol) (mPEG, Mn = 5,000, PDI = 1.03), stannous 2-ethylhexanoate (Sn(Oct)$_2$), and benzyl bromide were purchased from Sigma Aldrich (St. Louis, MO). Enzyme color endpoint assay kit for alanine aminotransferase (ALT) and aspartate aminotransferase (AST) were purchased from ID Labs™ Inc. (London, ON, Canada), and rat TNF-α ELISA, total bilirubin (BIL) detection kit from Bio scientific (Austin, TX). Radioimmunoprecipitation assay (RIPA) buffer was purchased from (Roche, Indianapolis, IN). L-lactide (LA) was purchased from PURAC Biochem BV (Gorinchem, Netherlands) and recrystallized from ethyl acetate. All other reagents were obtained from Sigma Aldrich and used without further purification.

Synthesis and Characterization of mPEG-b-P(CB-co-LA)

mPEG-b-p(CB-co-LA) copolymer was synthesized by ring opening polymerization (ROP) as described previously (13). Briefly, mPEG, 5-methyl-5-benzyloxycarbonyl-1,3-dioxane-2-one (MBC) and L-lactide were taken at a ratio of 1:2.5:2.5, respectively to synthesize a copolymer of targeted average molecular weight of 30 kDa. Sn(Oct)$_2$ (10 mol% relative to mPEG) was used as a catalyst for the reaction. The mixture was stirred for 24 h at 130°C under vacuum. After cooling, the product was dissolved in chloroform and purified by precipitation in excess of diethyl ether and hexane (1:2). The copolymer was characterized by ^{1}H NMR and spectra were recorded with a Varian (500 MHz, T = 25) using deuterated dimethyl sulfoxide (DMSO-d6) as solvent. Chemical shifts were calibrated using tetramethylsilane as an internal reference and given in parts per million.

Preparation of Nanoparticles

Nanoparticles were prepared using mPEG-b-p(CB-co-LA) copolymer by the emulsion/solvent evaporation technique (14). Briefly, 30 mg copolymer was dissolved in dichloromethane and acetone mixture (50:50) containing 1.5 mg GDC or 0.6 mg RSG. For combination therapy, nanoparticles carrying both GDC and RSG were prepared by dissolving both these two drugs with copolymer in dichloromethane and acetone mixture. The solution was then added to a vial containing 5 ml of 1% aqueous poly (vinyl alcohol) solution and emulsified by a probe sonicator (50 W, 2 min) on ice bath. Organic solvents were evaporated under vacuum. Nanoparticles were collected by ultracentrifugation at 25,000 rpm for 35 min, (Du point, Sorvall Inc.), washed three times with distilled water and lyophilized.

Characterization of Nanoparticles

Mean particle size and size distribution of the nanoparticles were determined by dynamic light scattering using a Zeta Sizer™ (Malvern 3800-ZLS, Boston, MA). Drug loading

and encapsulation efficiency was determined using HPLC analysis. Briefly, GDC and RSG loaded nanoparticles with 0.5 mg theoretical drug loading were dissolved in DCM for drug extraction using a bath sonicator for 30 min at 37°C. DCM was evaporated and acetonitrile was added to dissolve residues. Drug content was determined by HPLC (Waters, MA) by using a reverse phase C-18 Inertsil ODS column (150 mm×4.6 mm, 5 µm) (GL Sciences Inc.). Mobile phase composition was acetonitrile and 10 mM acetate buffer (pH 4.5) (60/40, v/v) at a flow rate of 1.0 ml/min. Detection wavelength of 330 nm and 254 nm were used for GDC and RSG, respectively. Drug loading and encapsulation efficiency were calculated using the following equations:

$$\text{Encapsulation efficiency}(\%) = \frac{\text{weight of drug encapsulated}}{\text{initial weight of drug taken}} \times 100$$

$$\text{Drug loading }(\%\,w/w) = \frac{\text{weight of drug encapsulated}}{\text{total weight of formulation}} \times 100$$

In Vitro Drug Release

Drug-loaded nanoparticles containing 1 mg of GDC and 0.5 mg of RSG were placed in a dialysis bag with a molecular weight cutoff of 1,000 Da (Spectrum Labs Inc., Rancho Dominguez, CA). Dialysis bag were suspended in 50 mL of PBS (pH 7.4) containing 1.0% (w/w) Tween 80 to facilitate drug wetting and to maintain the sink conditions. Study was performed in a closed chamber orbital shaker at 37°C, with a rotation speed of 100 rpm. Samples (1 mL) were taken at regular time intervals and replaced with the PBS (pH 7.4) containing 1.0% (w/w) Tween 80. Drug content in the samples was analyzed by HPLC-UV method as described above and cumulative drug release was plotted against time.

Animal Experiments

Animal experiments were performed in accordance with the NIH guidelines using a protocol approved by the Institutional Animal Care and Use Committee (IACUC) of the University of Tennessee Health Science Center. Male Sprague Dawley (SD) rats weighing 230–250 g were purchased from Charles River Laboratories, Inc. (Wilmington, MA), housed under the care of a licensed veterinarian and monitored daily for signs of sickness or pain after surgery. The animals were maintained on a 12-h light–dark schedule and had free access to normal rat chow and water. To induce liver fibrosis, common bile duct of SD rats was ligated as described previously (15). Animals were divided into the following five groups (5 per group): control (sham operated), CBDL untreated, CBDL treated with GDC loaded nanoparticles at a dose of 10 mg/kg, CBDL treated with RSG loaded nanoparticles at a dose of 4 mg/kg, and CBDL treated with nanoparticles loaded with GDC and RSG at a dose of 5 mg/kg and 2 mg/kg of GDC and

RSG respectively. Nanoparticles containing GDC, RSG and both drugs were administered daily after 3 days of CBDL via intravenous tail vein injection for a week. Animals were euthanized under isoflurane anesthesia at the end of the study to collect serum and liver tissues. Serum was used for biochemical analysis and the liver was fixed in 10% neutral buffered formalin or snap frozen in liquid nitrogen for further analysis.

Measurement of Serum Enzyme Levels and Liver Histology

Serum concentrations of liver injury markers such as ALT, AST and BIL were measured using standard assay kits according to the manufacturer's instructions. For staining, liver specimens were fixed in 10% buffered formalin overnight, saturated in 30% sucrose solution and embedded in OCT (optimum cutting temperature) compound. For standard histology, 5 µm thick sections were stained with Hematoxylin–Eosin (H&E) for detection of tissue architecture. Masson's trichrome staining was used to determine the levels of collagen deposition.

Immunofluorescent Staining

For immunofluorescent staining, snap frozen liver sections were fixed on glass slides in 95% cold ethanol for 10 min and blocked with 10% goat serum. This was followed by overnight incubation at 4°C with polyclonal antibodies for TGF-β1, Gli-1, (Santa Cruz, CA), and α-SMA (Abcam, Cambridge, MA). After washing with tris-buffered saline containing (0.05% w/w) Tween 20 (TBST), slides were incubated with anti-rabbit or anti-goat secondary antibodies (IgG - H&L DyLight® 488 (Abcam) for 2 h at room temperature and visualized under a fluorescent microscope.

Quantitative RT-PCR

Total RNA was extracted from the liver tissues using RNeasy Mini Kit (Qiagen, MD) and reverse transcribed to cDNA using Taqman RT kit (Carlsbad, CA). Gene expression levels were determined by Light Cycler 480 (Roche, IA) using primer pairs (Table I) and standard protocol as described previously (9). All the real time RT-PCR results were analyzed using comparative CT method and gene expression was normalized as compared to the control.

Western Blot Analysis

Snap frozen liver tissues were homogenized in RIPA buffer containing protease inhibitor cocktail to extract total protein. After resolving in sodium dodecyl sulfate-polyacrylamide gel

Table I Primers Sequences Used for Real Time RT-PCR Amplification

GENE	NCBI accession #	Sequence
β- actin	NM_031144	CAACTGGGACGATATGGAGAAG (Sense)
		CTCGAAGTCTAGGGCAACATAG (Antisense)
Shh	NM_017221	CTGGATTCGACTGGGTCTACTA (Sense)
		GCTTTCCCGGTTGCTTATCT (Antisense)
Ptch-1	NM_053566	CAAAGCCAAGGTTGTGGTAATC (Sense)
		GCGGTCAGGTAGATGTAGAAAG (Antisense)
Gli-1	NM_001191910.1	ACCTCCCTACCTCTGTCTATTC (Sense)
		GGCAGGATAGGAGACTGATTTG (Antisense)
SMO	NM_012807	CCAGGACATGCACAGTTACA (Sense)
		GGAAGTAGCCTCCCACAATAAG (Antisense)
α-SMA	NM_031004.2	CTGGCACCACTCCTTCTATAAC (Sense)
		CTCCAGAGTCCAGCACAATAC (Antisense)
IL-6	NM_012589	CCGTTTCTACCTGGAGTTTGT (Sense)
		GTTTGCCGAGTAGACCTCATAG (Antisense)
TGF-β1	NM_021578.2	CTGTGGAGCAACACGTAGAA (Sense)
		GGGTGCAGGTGTCCTTAAATA (Antisense)
E-cadherin	NM_031334.1	AAGAGGGAGGTGGAGAAGAA (Sense)
		ACAGACAGACTGGTAGGTAGAG (Antisense)
PPAR-γ	NM_013124.3	CTGGCCTCCCTGATGAATAAAG (Sense)
		GCGGTCTCCACTGAGAATAATG (Antisense)
TNF-α	NM_012675	CAGCCGATTTGCCATTTCATAC (Sense)
		GGCTCTGAGGAGTAGACGATAA (Antisense)
FN-1	NM_019143.2	GTGTCCTCCTTCCATCTTCTTAC (Sense)
		GTTCCCTCTGTTGTCCTTCTT (Antisense)
COL1A1	NM_053304.1	CGGACTATTGAAGGAGCCTAAC (Sense)
		TGATGCAGGACAGAGAGAGA (Antisense)

electrophoresis (SDS-PAGE), proteins were transferred to Immobilon polyvinylidene fluoride membrane using iBlot™ Dry Blotting System (Invitrogen, Carlsbad, CA). Transferred membranes were blocked in Odyssey blocking buffer and incubated with Shh, Gli-1, FN-1, NF-κB, α-SMA, TGF-β1 and PPAR-γ primary antibodies for 16 h at 4°C. Membrane was then incubated with anti-goat or anti-rabbit IRDye 680RD secondary antibodies for 1 h at room temperature. All the blots were re-probed with total β-actin antibody as control. Target proteins were imaged using Odyssey IR imaging system (Li-Cor, Lincoln, NE).

ELISA for Tumor Necrosis Factor-α

TNF-α in rat serum was determined according to the manufacturer's instructions of ELISA kit. Briefly, ELISA plate provided in the kit was coated with capture antibody overnight at 4°C. Plate was washed and blocked with assay diluent and incubated at room temperature for 1 h. Rat serum samples were added and incubated at 4°C overnight. After washing, detection antibody was added and incubated at

room temperature for 1 h. Avidin-HRP conjugated secondary antibody was added and incubated at room temperature for 30 min. Plate was washed and substrate solution was added to each well and read at 450 nm.

Statistical Analysis

All values in the figures and text were expressed as the mean ± S.D. The results were analyzed and individual group means were compared using Student's unpaired t-test. A p-value of at least 0.05 was considered statistically significant.

RESULTS

Preparation and Characterization of Drug-Loaded Nanoparticles

We synthesized $mPEG_{114}$-b-p(CB_{55}-co-LA_{160}) triblock amphiphillic copolymer and characterized it by ^1H NMR. The polymer had an average molecular weight of 30,000 Da

with carbonate and lactic acid contents of 55 ± 5 and 160 ± 5 moles, respectively, and mPEG content of $16.6\pm2\%$ as determined by ^{1}H NMR (Fig. 1a).

Using the above synthesized copolymer, we were able to formulate nanoparticles with a mean particle size of 120–130 nm and a polydispersity index of less than 0.2 (Fig. 1b). Drug loading was found to be 5.0% and 2.0% w/w for GDC and RSG, respectively, with little effect on the mean particle size and size distribution. The encapsulation efficiency was 98% and 95% for GDC and RSG, respectively. Nanoparticles carrying these two drugs were prepared using half of 5% & 2% theoretical drug loading with encapsulation efficiencies of 95% and 90% for GDC and RSG, respectively (Fig. 1c).

In vitro release profile of drug-loaded nanoparticles was determined in PBS at 37°C. Nanoparticles carrying GDC and RSG followed Higuchi model with $80\pm2.7\%$ release in 10 days and $96\pm3.1\%$ in 4 days cumulative release for GDC and RSG, respectively (Fig. 1d). At the end of the study, remaining unreleased drug was recovered from the dialysis bags. There was an initial burst release for about 5 h possibly due to the dissolution and diffusion of surface adsorbed and poorly entrapped drug in the nanoparticles.

Effect of Drug Treatment on Liver Histology

To treat CBDL induced fibrotic rats, drug-loaded nanoparticles were injected daily intravenously after 3 days of CBDL for a week. CBDL resulted in bile accumulation in bile duct, resulted in proliferation and enlargement of bile duct (16). In untreated CBDL rats, maximum proliferation was observed but reduced after intravenous injection of nanoparticles encapsulated with GDC, RSG or in combination. These results suggest that treatment with GDC and RSG improved the overall condition of these liver fibrotic rats.

CBDL is known to cause increase in intra-biliary pressure and leakage of bile into the liver parenchyma, which aggravates bile infarcts due to hepatocyte death (17). Liver specimens from CBDL rats demonstrated extensive bile infarcts, while the number and area of infarction was significantly reduced upon administration of GDC or RSG loaded nanoparticles as evident from H&E staining. These results suggest that Hh inhibitor and PPAR-γ agonist can attenuate liver injury and protect liver architecture (Fig. 2a).

Liver sections were stained with Masson's trichrome stain for collagen. The increased deposition of collagen was evident by intense blue color staining for the interstitial collagen in CBDL rats (Fig. 2b). However, collagen staining was much weaker when nanoparticles loaded GDC, RSG either alone or in combination were administered into CBDL rats, indicating significant inhibition of collagen accumulation in the enlarged periductal area and essentially no collagen accumulation in the liver interstitium.

Measurement of Liver Injury Markers

ALT, AST and BIL are surrogate markers for liver injury and their levels are known to increase upon bile duct ligation (18). As evident from Fig. 3, CBDL rats had many fold increase in serum AST, ALT and BIL levels as compared to the sham operated control rats. Treatment with GDC and RSG loaded

Fig. 1 Polymer synthesis, formulation and characterization of nanoparticles. (**a**) ^{1}H NMR spectra of mPEG$_{114}$-b-p(CB$_{54}$-co-LA$_{160}$) copolymer in DMSO-d6. (**b**) Particle size distribution of nanoparticles. (**c**) Polydispersity index (PDI), Drug encapsulation efficiency (EE) and loading efficiency (LE) of nanoparticles. (**d**) Release of GDC and RSG from nanoparticles at 37°C by dialysis in PBS (pH 7.4) containing 1.0% Tween 80. All data are presented as the mean ± S.D. ($n=3$).

| Batch	Size (nm)	PDI	EE (%)	LE (%)
GDC	130±10	0.17	95.40	5
RSG	131±10	0.13	90.76	2
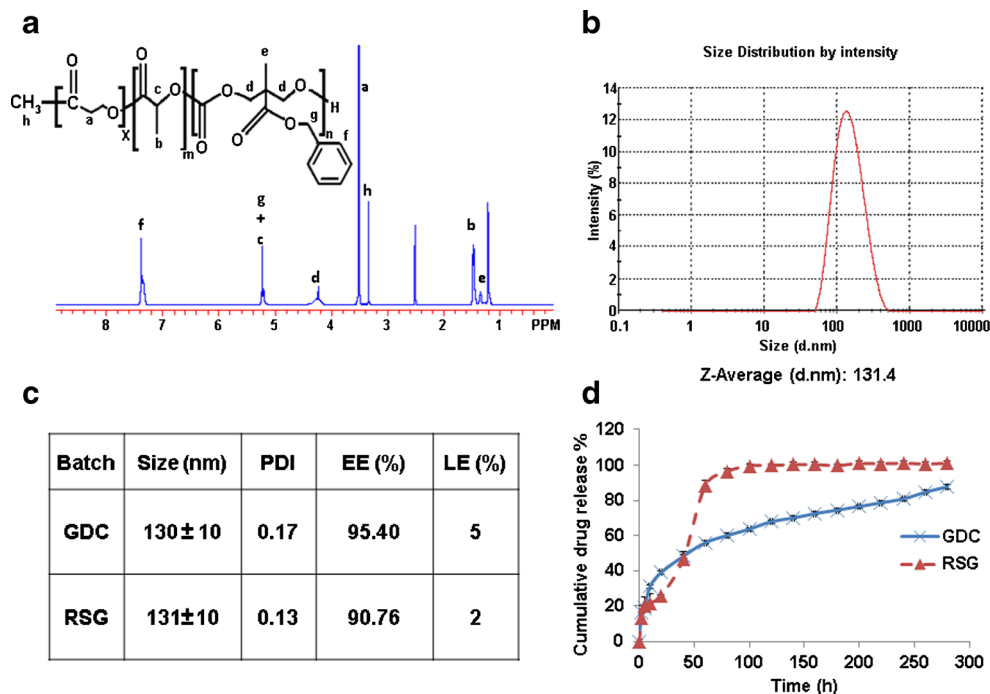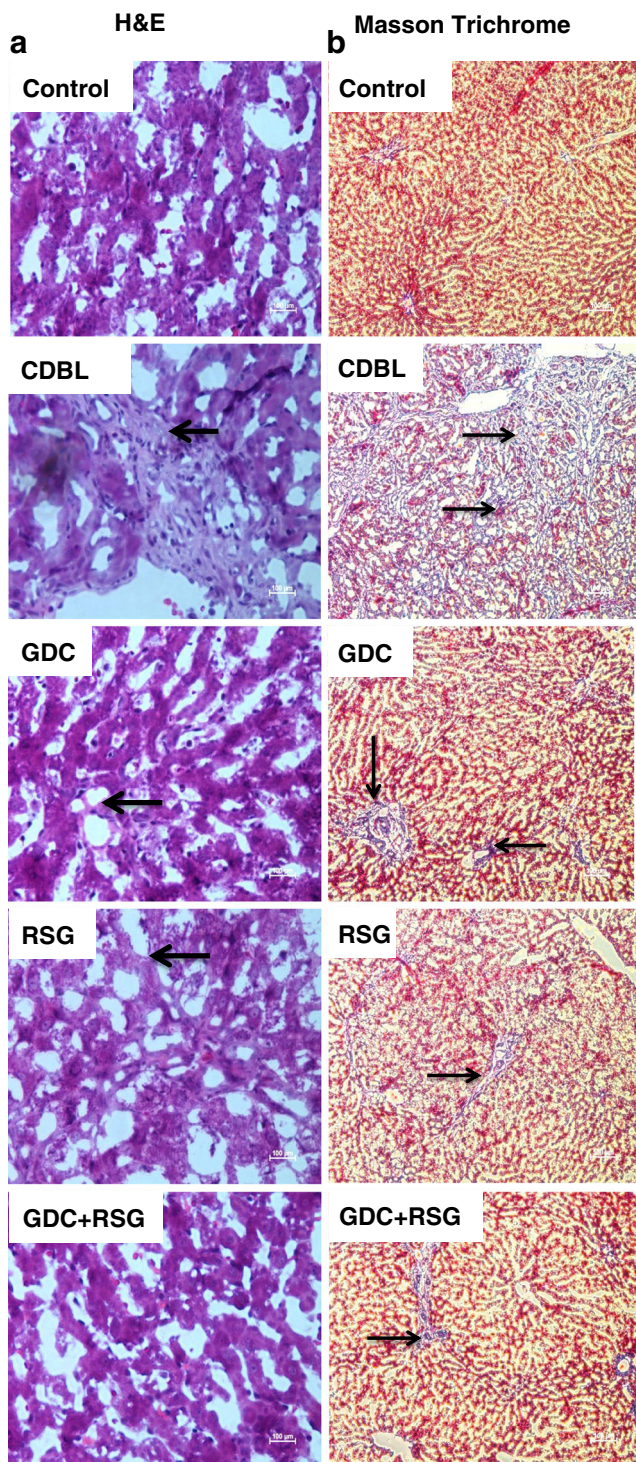
Fig. 2 Hematoxylin & Eosin and Masson trichrome staining of liver sections of CBDL rats after systemic administration of nanoparticles loaded with GDC, RSG or combination. (**a**) Treatment with GDC and RSG loaded nanoparticles reduced histological liver injury, including bile infarcts. Geographic borders of infarcts indicated by black arrows were large in number and area in untreated CBDL rats and reduced upon treatment with nanoparticles carrying GDC and RSG (original magnification ×20). (**b**) *Dark blue* staining shows increased collagen deposition in CBDL rats (*Black Arrows*). Systemic administration of GDC and RSG loaded nanoparticles effectively reduced blue collagen staining (original magnification, ×10).

nanoparticles resulted in decreased serum levels of all of these markers. These results indicate that the liver is susceptible to hepatocellular injury following CBDL, and GDC and RSG loaded-nanoparticles protected livers from the injury resulting in significant decrease in ALT, AST, and BIL (Fig. 3,**$P < 0.005$).

Expression Levels of Hh Ligand and PPAR-γ

Hh signaling controls proliferation and migratory activities of Hh-responsive HSCs by promoting EMT (1). Therefore, we measured Hh pathway ligands expression in CBDL rats after 7 days of systemic administration of GDC or RSG loaded nanoparticles and compared with the sham operated control by RT-PCR and Western blotting method. Shh mRNA was increased by 4.3 folds in CBDL rat livers. There was also significant increase in transcription of Ptch-1 by 2.7 folds, SMO by 2.8 folds and Gli-1 by 3.6 folds as compared to the
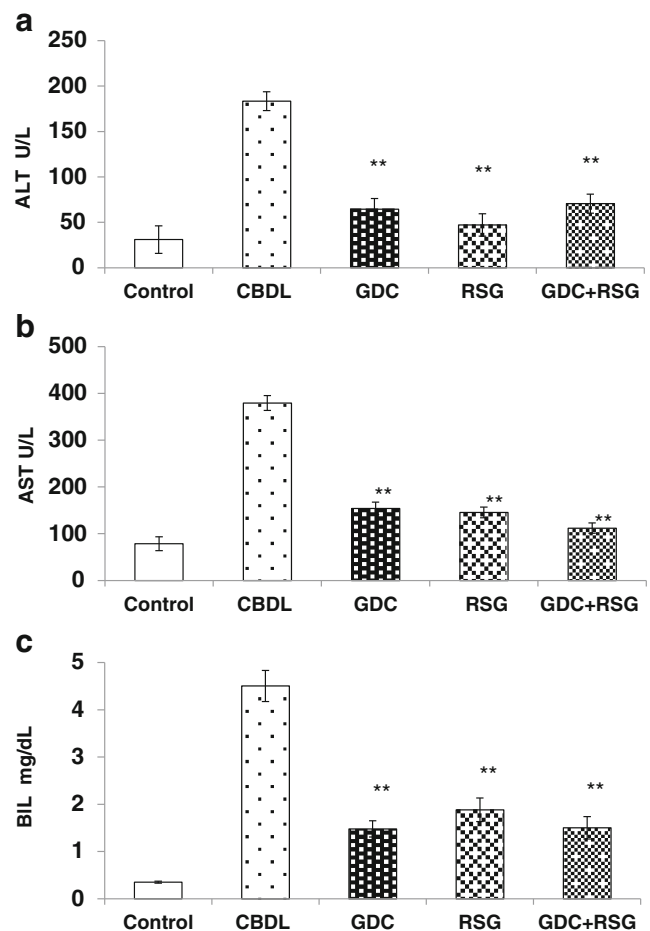
Fig. 3 Serum biomarkers. Effect of GDC and RSG loaded nanoparticles on serum (**a**) AST, (**b**) ALT and (**c**) BIL levels. Serum markers in CBDL rats after systemic administration of GDC and RSG loaded nanoparticles were significantly lower than those in the CBDL rats. Results are presented as mean ± S.D. ($n = 5$); (**$p < 0.001$ treated rats as compared to CBDL).

control (Fig. 4a). Systemic administration of GDC loaded nanoparticles significantly decreased Shh expression levels. Ptch-1, SMO and Gli-1 expressions were also significantly reduced in the liver when CBDL rats received nanoparticles carrying GDC alone or with RSG. Decrease in mRNA expression of Shh and Gli-1 was confirmed by Western blot analysis of liver tissue protein extract (Fig. 4b).

In contrast to Hh signaling, PPAR-γ mRNA was significantly downregulated in CBDL rat livers, which is in good agreement with the literature (7). Treatment of CBDL rats with RSG-loaded nanoparticles significantly restored PPAR-γ gene expression to the basal level (Fig. 4c). These results were also confirmed by Western blot analysis (Fig. 4d).

Progression of liver fibrosis leads to an increase in the synthesis and deposition of extracellular matrix (ECM) proteins, particularly collagen in the liver interstitium (19). We determined mRNA expression level of collagen type-I (COL1A1) and observed 4.7 folds higher expression in the CBDL rats as compared to the control, but its expression decreased upon treatment with nanoparticles carrying GDC (1.48 fold) or RSG alone (1.8 fold) or combination (1.34 fold) which is consistent with the results observed in Masson's trichrome staining (Fig. 5a).

α-SMA and FN-1 are characteristic markers of EMT (20). Therefore, we determined transcription levels of α-SMA and FN-1 and found upregulation of their expression by 2.3 and 3.2-folds, respectively in CBDL rats (Fig. 5a). After systemic administration of nanoparticles carrying GDC or RSG either alone or in combination into CBDL rats, α-SMA and FN-1 expression decreased significantly both at mRNA and protein level (Fig. 5a, b). NF-kB promotes the secretion of inflammatory factors and its expression is known to be elevated in liver fibrosis (5). We found its level elevated in CBDL rats and upon treatment with nanoparticles containing drugs decreased its protein level (Fig. 5b). TGF-β1 is involved in early proliferation of HSCs through SMAD3 /SMAD2 signaling after CBDL (21). Similarly, TGF-β1 expression was upregulated (3.64 folds) at mRNA level and significantly increased at proteins levels after CBDL, and was decreased in GDC or RSG alone or in combination treatment groups to basal level (Fig. 5a, b). E-cadherin is a transmembrane glycoprotein found in most epithelial cells, and promotes cell adhesion by forming a complex with β-catenin. Upon EMT, epithelial cells lose E-cadherin expression (22). Therefore, we determined E-cadherin expression and found its expression was decreased to 40% in CBDL rats as compared to the sham operated control rats. After treatment with nanoparticles carrying GDC or RSG alone or in combination we observed significant increase in its mRNA level (Fig. 5c).

Expression of Proinflammatory Cytokines

Increased TGF-β1 induces IL-6 secretion at the site of injury (23). We observed mRNA levels of IL-6 to be significantly upregulated in CBDL rats compared to the control rats. Significant down regulation of IL-6 mRNA was seen in the CBDL rats treated with GDC and RSG loaded nanoparticles (Fig. 4c). Moreover, we determined TNF-α expression which is an important proinflammatory cytokine in progression of liver injuries and fibrosis (24). RT-PCR and ELISA results showed TNF-α mRNA and protein levels were significantly higher in CBDL rats as compared to the sham operated control rats. Upon systemic administration of nanoparticles loaded with GDC or RSG alone or combination to CBDL rats resulted in reduced TNF-α gene expression at both mRNA and protein level (Fig. 6a, b).

Immunofluorescent Staining

Immunofluorescence for Hh-regulated transcription factor, Gli-1 overexpression was localized in the nucleus of Hh-responsive cell population. This observation suggests that Hh ligands are highly activated in CBDL rats, resulting in intense immunofluorescent staining of Gli-1. However, Gli-1 expression was significantly reduced in CBDL rats after systemic administration of nanoparticles carrying GDC alone or with RSG (Fig. 7a).

Immunoreactivity of mesenchymal cell markers, α-SMA and TGF-β1 correlate well with the progression of liver fibrosis. Immunofluorscent staining of the liver sections indicate that CBDL rats have increased number of α-SMA expressing myofibroblasts in and around portal tracts (Fig. 7b). TGF-β1 positive cells were distributed with high density in the portal venule pericytes with perisinusoidal distribution. Treatment groups showed decreased number of α-SMA and TGF-β1 producing cells in CBDL rats treated with nanoparticles carrying GDC or RSG. However, there was still fair a number of TGF-β1-positive cells in the liver sections of CBDL rats treated with GDC or RSG loaded nanoparticles, which distributed mainly at the fibrous septa band (Fig. 7c).

DISCUSSION

Liver fibrosis is affecting millions of people and is a significant cause of morbidity and mortality worldwide. Liver fibrosis is the result of wound-healing response to the liver injury, viral hepatitis or biliary tract disease. Fibrosis is characterized by the excessive production and deposition of ECM proteins. Chronic liver injuries result in the transformation of quiescent HSCs into active myofibroblasts (25). Initiation and progression of liver fibrosis involves multiple regulatory events in the liver and coordinated changes in the activity of several transcription factors. A number of different approaches have been used earlier for treatment, including the inhibition of collagen synthesis, interruption of matrix deposition, stimulation of matrix degradation, modulation of HSC activation, induction

Fig. 4 RT-PCR and Western blot analysis of hedgehog ligands and PPAR-γ. (**a**) Systemic administration of GDC loaded nanoparticles into CBDL rats reduced gene expressions of Shh, Gli-1, Smo and Ptch-1 as quantified by Real-Time RT-PCR. (**b**) Western blot analysis of liver tissues for Shh and Gli-1 proteins levels (**c**) mRNA expression levels of PPAR-γ and IL-6. (**d**) Western blot analysis of PPAR-γ protein. β-actin was used as an internal control. Results are presented as mean ± S.D. (n = 3) (**p < 0.001 Treated vs CBDL).
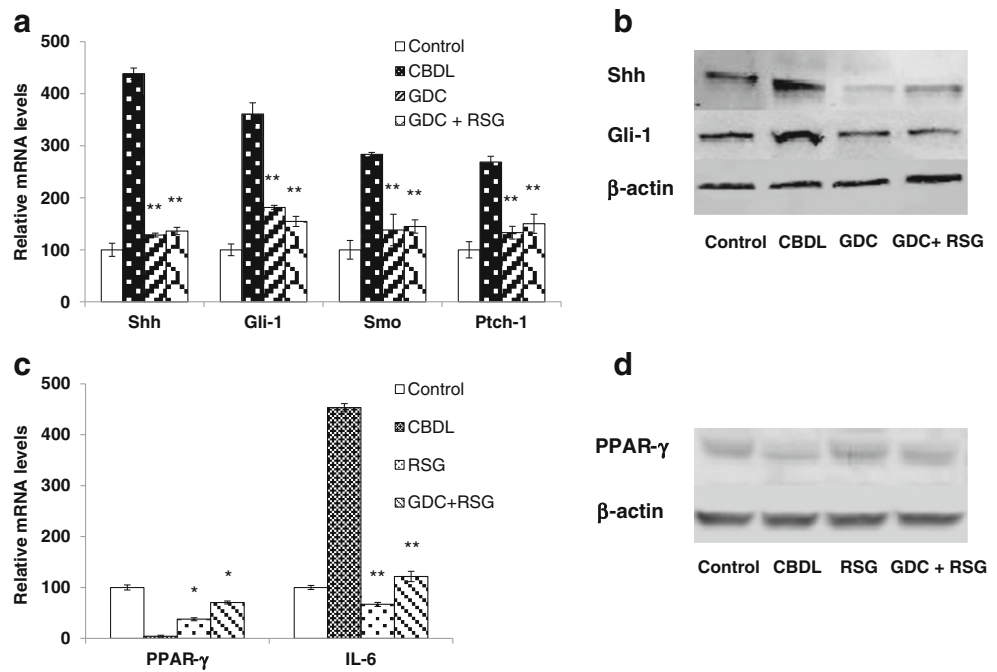
of HSC apoptosis and modulation of immune responses at the affected site (9,26–30). However, the complexity and rapid progression of the disease requires the use of multipronged approach by targeting more than one factor. PPAR-γ is one of the key factors whose activity is decreased in activated HSCs. On the other hand, there is an increase in Hh activity in fibrotic livers. Therefore, inhibition of inflammation and

EMT by combining of PPAR-γ agonist and Hh inhibitor can be a potential strategy to reverse liver fibrosis.

PPAR-γ agonist keeps HSCs in quiescent state by blocking the profibrotic effects of TGF-β1 and reducing TNF-α activity. Thus, the loss of these receptors leads to trans-differentiation of HSCs from the retinoid storing state to the ECM-producing myofibroblasts (7,31,32). RSG is a PPAR-γ

Fig. 5 RT-PCR and Western blot analysis of liver fibrosis markers. Systemic administration of RSG and GDC nanoparticles into CBDL rats reduced gene expression of Col1A1, α-SMA, FN-1 and TGF-β1. (**a**) RT-PCR (**b**) Western blot analysis of TGF-β1, α-SMA, FN-1 and NF-κB proteins from liver tissues of various groups. (**c**) RT-PCR of E-cadherin. Results are presented as mean ± S.D. (n = 3) (*p < 0.05, **p < 0.001, Treated vs CBDL).
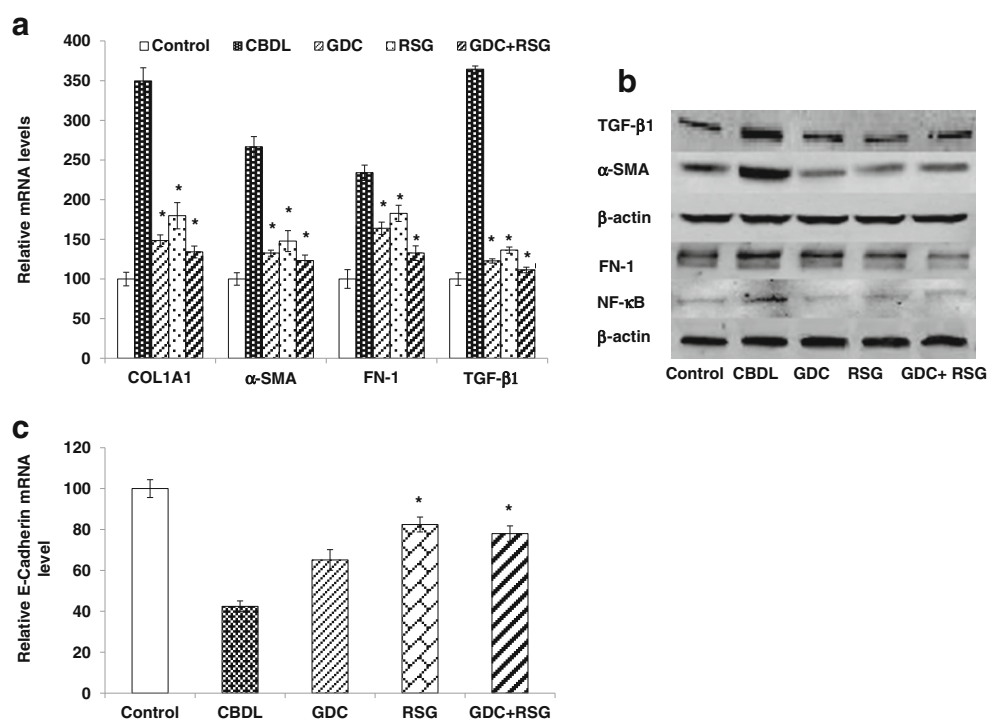
Fig. 6 RT-PCR and ELISA of inflammatory cytokine TNF-α. (**a**) mRNA level. (**b**) Serum TNF- α level. Results are presented as mean ± S.D. ($n = 3$) (**$p < 0.001$ Treated vs CBDL).
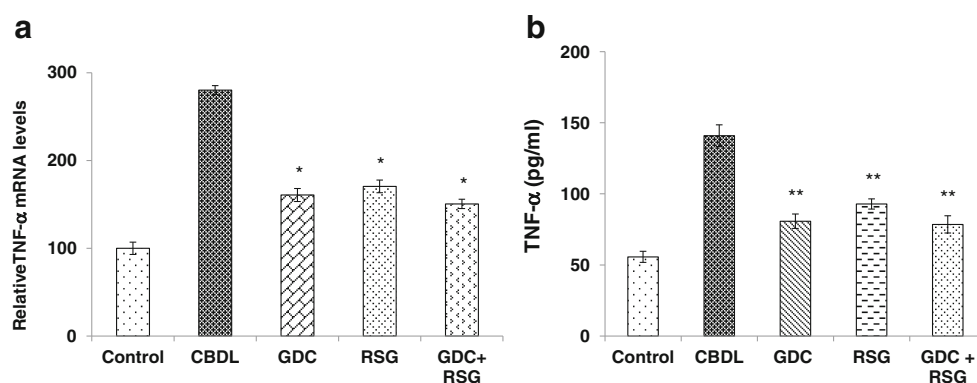
agonist which is a thiazolidinediones derivative used as an anti-hyperglycemic agent (33). In this study, RSG was chosen because it is non-toxic to the liver and does not induce cytochrome enzymes, like other members of this family (34).

Previously, we found that the progression of liver fibrosis is accompanied by the activation of Hh pathway leading to the proliferation and EMT of HSCs (8). Treatment with hedgehog inhibitor, GDC ameliorated fibrotic condition in CBDL rats (9). However, administration of GDC required complex formation with β-CD (beta-cyclodextrin) at low pH range, which is not suitable for systemic administration. Moreover, GDC shows poor complex formation withβ-CD.

Taking care of their poor aqueous solubility and potential side effects of GDC and RSG, in this study we aimed at formulating nanoparticles encapsulating these two]drugs using mPEG-b-p(CB-co-LA) copolymer. First we synthesized amphiphillic mPEG-b-p(CB-co-LA) copolymer and characterized it using ^{1}H NMR (Fig. 1a). We have selected this copolymer because of its capacity to encapsulate poor water soluble drugs with high drug loading, biodegradable and nontoxic properties (13). We have simultaneously encapsulated these drugs into nanoparticles successfully and tested this combination at half of their individual doses for treating liver fibrosis for minimizing any drug related toxicity.

These nanoparticle were not specifically targeted to the liver, however our group previously reported that micelles prepared from similar backbone copolymer PEG block-poly(2-methyl-2-benzoxycarbonyl-propylenecarbonate) tend to accumulate in the liver and spleen. (35). Based on these results, we expect nanoparticles containing GDC or RSG to be having same biodistribution profiles.

Drug-loaded nanoparticles were formulated using o/w emulsification followed by solvent evaporation. Using this copolymer, we formulated uniform size distributed nanoparticle with high drug loading (Fig. 1b and c). The outer coating shell of mPEG prevents particles from aggregation and also provides stealth properties. This is necessary for nanoparticles to escape from the reticuloendothelial system (RES) and prolong systemic circulation. Owing to the differences in their

hydrophobicity, their loading capacity in the formulated nanoparticle was different. At higher payload, the encapsulation capacity of both drugs decreseed, which may be due to the saturation of inner hydrophobic core. Nanoparticles carrying GDC and RSG were prepared at 5% and 2% w/w initial drug loading of GDC and RSG respectvely. Drug-loaded nanoparticles had a mean particle size of 130–140 nm. Nanoparticles provided sustained release with 80% drug release in 10 days and 96% in 4 days for GDC and RSG, respectively (Fig. 1d). We observed different release profile for these two drugs as GDC is more hydrophobic than RSG, and thus GDC had slower release rate. PBS containing 1.0% Tween 80 was used as release medium to maintain the sink conditions and to prevent drug precipitation upon release.

CBDL rats showed large infarcts and intense blue collagen staining, whereas systemic treatment with nanoparticles containing GDC, RSG or combination reduced number as well as area of infarcts and decreased intensity of collagen specific staining (Fig. 2a and b). Liver injury markers such as serum AST, ALT and BIL were found significantly elevated in CBDL rats as compared to GDC, RSG or combination nanoparticles treated rats (Fig. 3). A significant increase in Hh ligand and Gli-1 expression in CBDL rats was observed, as analyzed by RT-PCR, (Fig. 4a) Western blot analysis (Fig. 4b), and immunofluorescence (Fig. 7a). Upon systemic administration of GDC and RSG loaded nanoparticles to CBDL rats, significant decrease in HSC activation and liver fibrosis was observed.

There was significant decrease in PPAR-γ expression in CBDL rats as compared to the sham control. This reduction is related to upregulation of TNF-α, which is known to inhibit PPAR-γ expression (4). However, the treatment of CBDL rats with nanoparticles of RSG or in combination with GDC restored PPAR-γ expression at mRNA as well as protein levels, suggesting upregulation of this gene (Fig. 4c and d).

There was significant increase in TGF-β1 gene expression after CBDL in rats, possibly due to HSC activation (Figs. 5c and 7c). Moreover, activated HSCs show abundance of α-SMA proteins which is a well-known EMT
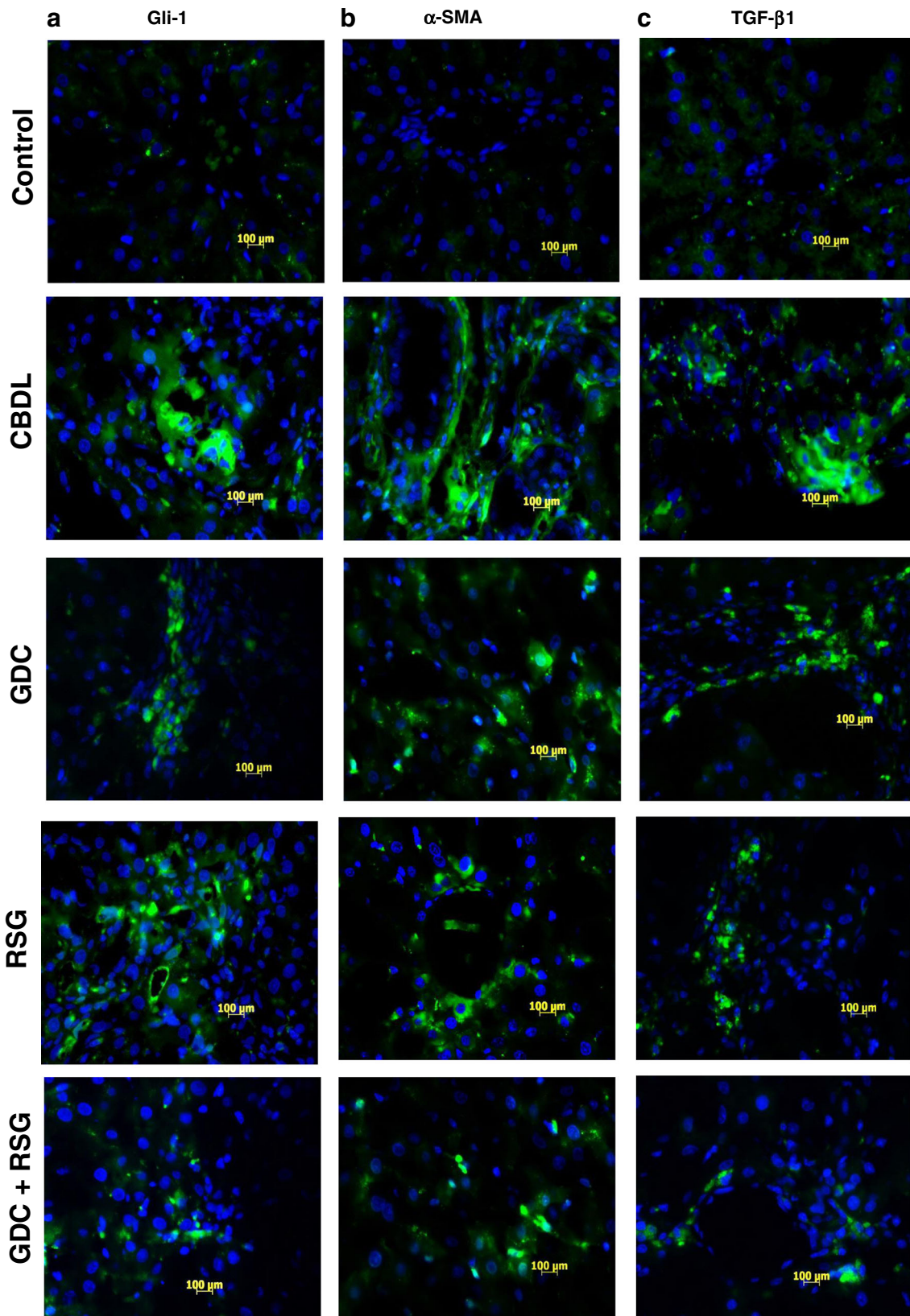
marker and used to identify the early stages of liver fibrosis (Figs. 5a, b and 7b) (36). Epithelial marker E-cadherin expression was decreased significantly in fibrotic livers (Fig. 5c). GDC and RSG carrying nanoparticles decreased

◀ Fig. 7 Immunofluorescent staining of liver sections: (**a**) Gli-1 expression in the liver sections of CBDL rats as reflected by intense green staining. GDC or combination treatment reduced Gli-1 expression as evident from faint green staining. (**b**) Sections from sham operated control rats do not express α-SMA, whereas CBDL rats showed strong fluorescent staining around the fibrous septa. α-SMA expression was decreased significantly after systemic administration of GDC and RSG loaded nanoparticles into CBDL rats. (**c**) Sham operated control rats showed weak staining for TGF-β1, whereas strong green staining can be seen in CBDL rats. Treatment groups showed weak staining for TGF-β1 as compared to CBDL group. Shown are representative images (original magnification, ×40).

TGF-β1 and α-SMA expression and also restored E-cadherin (Figs. 5 and 7b) suggesting nanoparticles loaded with these drugs have prevented EMT. FN-1 is among the first ECM proteins which is upregulated after liver injury, and mediates differentiation into myofibroblasts (37). After CBDL, upregulation of TGF-β1 also resulted in increased FN-1 expression (38). Treatment with GDC and RSG significantly abrogated FN-1 expression (Fig. 5a and b). Downregulation of these regulators is possibly the result of reduced activation of HSCs. Increase in collagen deposition was observed by Masson's trichrome staining and real-time RT-PCR . Following treatment with RSG and GDC carrying nanoparticles, reduced collagen level was observed in CBDL rats (Figs. 2b and 5c).

Upon liver injury, Kupffer cells increase TNF-α production via NF-κB pathway and its increased activity is found in activated HSCs"(5). TNF-α induces neutrophil infiltration and stimulates mitochondrial reactive oxygen species (ROS) production in hepatocytes. These reactive oxidants activate HSCs and stimulate inflammatory as well as fibrogenic signals (39). TNF-α was elevated in CBDL rats, which indicates high inflammatory state in the liver. RSG decreased the expression of genes implicated in the inflammation of liver tissues during the progression of liver fibrosis. RSG negatively interferes with NF-κB inflammatory pathway by blocking its nuclear translocation and by reducing the production of TNF-α (Fig. 6) and IL-6 (Fig. 4c).

CONCLUSION

In conclusion, mPEG-b-p(CB-co-LA) copolymer of 30, 000 Da was synthesized and GDC and RSG loaded nanoparticles were prepared. Systemic administration of nanoparticles encapsulating GDC and RSG provided hepatoprotection by reducing Hh pathway ligands and increasing PPAR-γ activity, respectively. GDC was more effective than RSG in treating experimental liver fibrosis when single drug was used. Combination therapy of GDC and RSG was able to treat early stage liver fibrosis even at a reduced dose and may provide a new strategy for treating liver fibrosis.

REFERENCES

1. Omenetti A, Porrello A, Jung Y, Yang L, Popov Y, Choi SS, *et al*. Hedgehog signaling regulates epithelial-mesenchymal transition during biliary fibrosis in rodents and humans. J Clin Invest. 2008;118: 3331–42.
2. Beachy PA, Karhadkar SS, Berman DM. Tissue repair and stem cell renewal in carcinogenesis. Nature. 2004;432:324–31.
3. Omenetti A, Diehl AM. The adventures of sonic hedgehog in development and repair. II. Sonic hedgehog and liver development, inflammation, and cancer. Am J Physiol Gastrointest Liver Physiol. 2008;294:G595–8.
4. Miyahara T, Schrum L, Rippe R, Xiong S, Yee Jr HF, Motomura K, *et al*. Peroxisome proliferator-activated receptors and hepatic stellate cell activation. J Biol Chem. 2000;275:35715–22.
5. Lueddeand T, Schwabe RF. NF-kappaB in the liver–linking injury, fibrosis and hepatocellular carcinoma. Nat Rev Gastroenterol Hepatol. 2011;8:108–18.
6. Omenetti A, Popov Y, Jung Y, Choi SS, Witek RP, Yang L, *et al*. The hedgehog pathway regulates remodelling responses to biliary obstruction in rats. Gut. 2008;57:1275–82.
7. Galli A, Crabb DW, Ceni E, Salzano R, Mello T, Svegliati-Baroni G, *et al*. Antidiabetic thiazolidinediones inhibit collagen synthesis and hepatic stellate cell activation in vivo and in vitro. Gastroenterology. 2002;122:1924–40.
8. Pratap A, Panakanti R, Yang N, Lakshmi R, Modanlou KA, Eason JD, *et al*. Cyclopamine attenuates acute warm ischemia reperfusion injury in cholestatic rat liver: hope for marginal livers. Mol Pharm. 2011;8:958–68.
9. Pratap A, Singh S, Mundra V, Yang N, Panakanti R, Eason JD, *et al*. Attenuation of early liver fibrosis by pharmacological inhibition of smoothened receptor signaling. J Drug Target. 2012;20:770–82.
10. Chen H, He YW, Liu WQ, Zhang JH. Rosiglitazone prevents murine hepatic fibrosis induced by Schistosoma japonicum. World J Gastroenterol WJG. 2008;14:2905–11.
11. Rudin CM, Hann CL, Laterra J, Yauch RL, Callahan CA, Fu L, *et al*. Treatment of medulloblastoma with hedgehog pathway inhibitor GDC-0449. N Engl J Med. 2009;361:1173–8.
12. Cheng-Laiand A, Levine A. Rosiglitazone: an agent from the thiazolidinedione class for the treatment of type 2 diabetes. Heart Dis. 2000;2:326–33.
13. Danquah M, Fujiwara T, Mahato RI. Self-assembling methoxypoly(ethylene glycol)-b-poly(carbonate-co-L-lactide) block copolymers for drug delivery. Biomaterials. 2010;31:2358–70.
14. Mundra V, Lu Y, Danquah M, Li W, Miller DD, Mahato RI. Formulation and characterization of polyester/polycarbonate nanoparticles for delivery of a novel microtubule destabilizing agent. Pharm Res. 2012;29:3064–74.
15. Panakanti R, Pratap A, Yang N, Jackson JS, Mahato RI. Triplex forming oligonucleotides against type alpha1(I) collagen attenuates liver fibrosis induced by bile duct ligation. Biochem Pharmacol. 2010;80:1718–26.
16. Wagner M, Fickert P, Zollner G, Fuchsbichler A, Silbert D, Tsybrovskyy O, *et al*. Role of farnesoid X receptor in determining hepatic ABC transporter expression and liver injury in bile duct-ligated mice. Gastroenterology. 2003;125:825–38.

17. Fickert P, Pollheimer MJ, Silbert D, Moustafa T, Halilbasic E, Krones E, et al. Differential effects of norUDCA and UDCA in obstructive cholestasis in mice. J Hepatol. 2013;58:1201–8.

18. Yamaura Y, Nakajima M, Takagi S, Fukami T, Tsuneyama K, Yokoi T. Plasma microRNA profiles in rat models of hepatocellular injury, cholestasis, and steatosis. PLoS ONE. 2012;7:e30250.

19. Yang N, Singh S, Mahato RI. Targeted TFO delivery to hepatic stellate cells. J Control Release Off J Control Release Soc. 2011;155:326–30.

20. Jiroutova A, Majdiakova L, Cermakova M, Kohlerova R, Kanta J. Expression of cytoskeletal proteins in hepatic stellate cells isolated from normal and cirrhotic rat liver. Acta Med. 2005;48:137–44.

21. Brantonand MH, Kopp JB. TGF-beta and fibrosis. Microbes Infect / Institut Pasteur. 1999;1:1349–65.

22. Chaw SY, Majeed AA, Dalley AJ, Chan A, Stein S, Farah CS. Epithelial to mesenchymal transition (EMT) biomarkers–E-cadherin, beta-catenin, APC and Vimentin–in oral squamous cell carcinogenesis and transformation. Oral Oncol. 2012;48:997–1006.

23. Seong GJ, Hong S, Jung SA, Lee JJ, Lim E, Kim SJ, et al. TGF-beta-induced interleukin-6 participates in transdifferentiation of human Tenon's fibroblasts to myofibroblasts. Mol Vis. 2009;15:2123–8.

24. Schwabe RF, Brenner DA. Mechanisms of Liver Injury. I. TNF-alpha-induced liver injury: role of IKK, JNK, and ROS pathways. Am J Physiol Gastrointest Liver Physiol. 2006;290:G583–9.

25. Rosenbloom J, Mendoza FA, Jimenez SA. Strategies for anti-fibrotic therapies. Biochim Biophys Acta. 2013;1832:1088–103.

26. Muriel P. Alpha-interferon prevents liver collagen deposition and damage induced by prolonged bile duct obstruction in the rat. J Hepatol. 1996;24:614–21.

27. Ye Z, Cheng K, Guntaka RV, Mahato RI. Receptor-mediated hepatic uptake of M6P-BSA-conjugated triplex-forming oligonucleotides in rats. Bioconjug Chem. 2006;17:823–30.

28. Bickel M, Baringhaus KH, Gerl M, Gunzler V, Kanta J, Schmidts L, et al. Selective inhibition of hepatic collagen accumulation in experimental liver fibrosis in rats by a new prolyl 4-hydroxylase inhibitor. Hepatology. 1998;28:404–11.

29. Iimuro Y, Nishio T, Morimoto T, Nitta T, Stefanovic B, Choi SK, et al. Delivery of matrix metalloproteinase-1 attenuates established liver fibrosis in the rat. Gastroenterology. 2003;124:445–58.

30. Wright MC, Issa R, Smart DE, Trim N, Murray GI, Primrose JN, et al. Gliotoxin stimulates the apoptosis of human and rat hepatic stellate cells and enhances the resolution of liver fibrosis in rats. Gastroenterology. 2001;121:685–98.

31. Wu CW, Chu ES, Lam CN, Cheng AS, Lee CW, Wong VW, et al. PPARgamma is essential for protection against nonalcoholic steatohepatitis. Gene Ther. 2010;17:790–8.

32. Yu J, Zhang S, Chu ES, Go MY, Lau RH, Zhao J, et al. Peroxisome proliferator-activated receptors gamma reverses hepatic nutritional fibrosis in mice and suppresses activation of hepatic stellate cells in vitro. Int J Biochem Cell Biol. 2010;42:948–57.

33. Hauner H. The mode of action of thiazolidinediones. Diabetes Metab Res Rev. 2002;18 Suppl 2:S10–5.

34. Balfour JA, Plosker GL. Rosiglitazone. Drugs. 1999;57:921–30. discussion 931–922.

35. Lu W, Li F, Mahato RI. Poly(ethylene glycol)-block-poly(2-methyl-2-benzoxycarbonyl-propylene carbonate) micelles for rapamycin delivery: in vitro characterization and biodistribution. J Pharm Sci. 2011;100:2418–29.

36. Carpino G, Morini S, Ginanni Corradini S, Franchitto A, Merli M, Siciliano M, et al. Alpha-SMA expression in hepatic stellate cells and quantitative analysis of hepatic fibrosis in cirrhosis and in recurrent chronic hepatitis after liver transplantation. Dig Liver Dis Off J Ital Soc Gastroenterol Ital Assoc Study Liver. 2005;37:349–56.

37. Olsen AL, Sackey BK, Marcinkiewicz C, Boettiger D, Wells RG. Fibronectin extra domain-A promotes hepatic stellate cell motility but not differentiation into myofibroblasts. Gastroenterology. 2012;142:928–37. e923.

38. Guo B, Koya D, Isono M, Sugimoto T, Kashiwagi A, Haneda M. Peroxisome proliferator-activated receptor-gamma ligands inhibit TGF-beta 1-induced fibronectin expression in glomerular mesangial cells. Diabetes. 2004;53:200–8.

39. Maher JJ, Zia S, Tzagarakis C. Acetaldehyde-induced stimulation of collagen synthesis and gene expression is dependent on conditions of cell culture: studies with rat lipocytes and fibroblasts. Alcohol Clin Exp Res. 1994;18:403–9.